Supporting Information

Uncovering the Determinants of a Highly Perturbed Tyrosine pK_a in the Active Site of Ketosteroid Isomerase

Jason P. Schwans, Fanny Sunden, Ana Gonzalez, Yingssu Tsai, and Daniel Herschlag

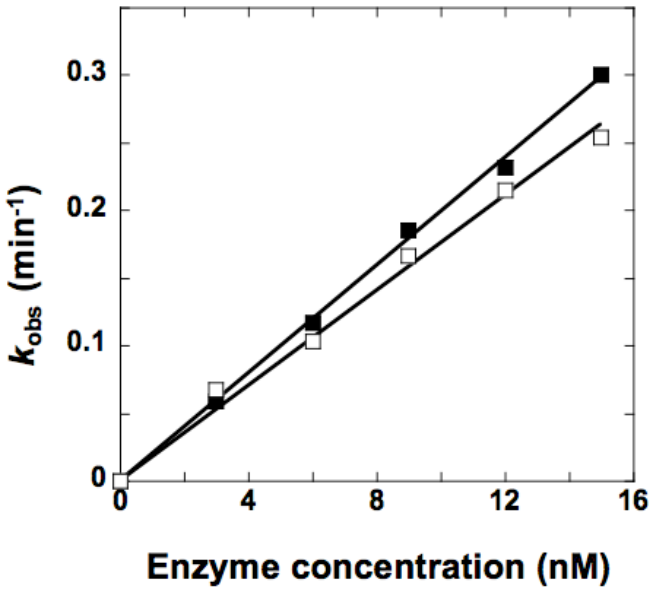

Figure S1. Effect of the R15K/D21N/D24C mutations on KSI activity. Activity of wild type-KSI (■) and R15K/D21N/D24C (□) using subsaturating concentrations of 5(10)-estrene-3,17-dione. k_{cat}/K_M = 3.3×10^5 and 2.9×10^5 $M^{-1}s^{-1}$ for wild type-KSI and R15K/D21N/D24C, respectively.

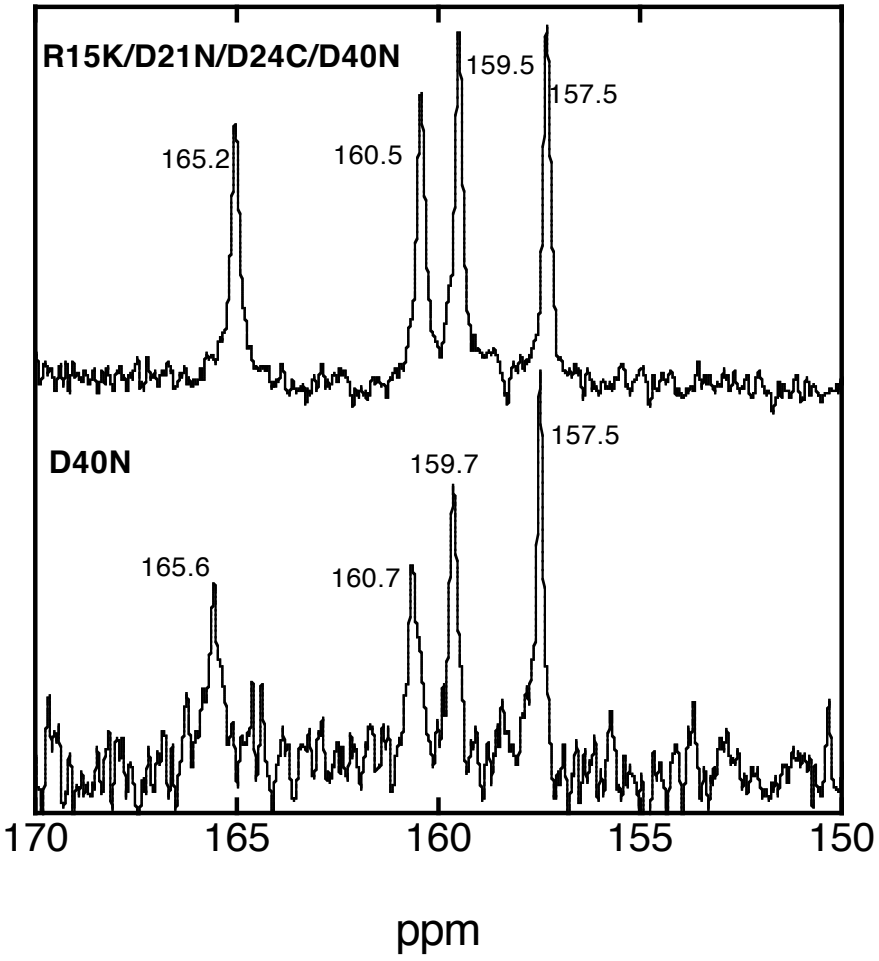

Figure S2. NMR spectra of D40N and D40N enzyme bearing mutations for semi-synthesis (R15K/D21N/D24C/D40N). Spectra were acquired as described in the Experimental Section.

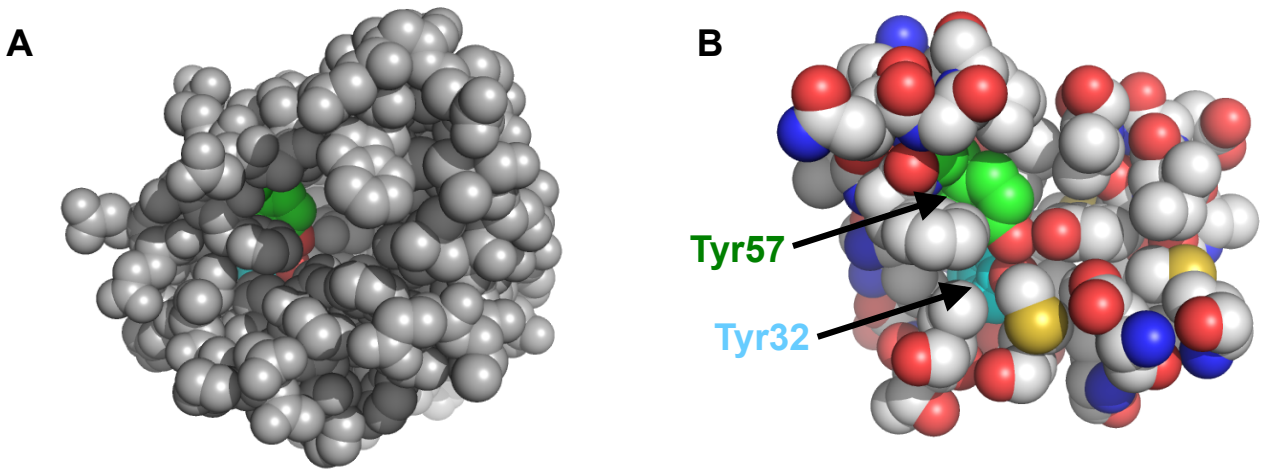

Figure S3. Space filling representation of KSI (PDB ID 1OPY) showing the location of Tyr57 and Tyr32 in the active site. (**A**) Space filling representation of the KSI monomer shows that Tyr57 (carbon atoms colored green) is on the solvent accessible surface whereas Tyr32 is excluded from solvent (carbon atoms cyan). (**B**) Close-up space filling representation of the residues surrounding Tyr57 and Tyr32. The carbon atoms of the surrounding residues are colored grey and Tyr57 and Tyr32 are colored as in panel **A**.

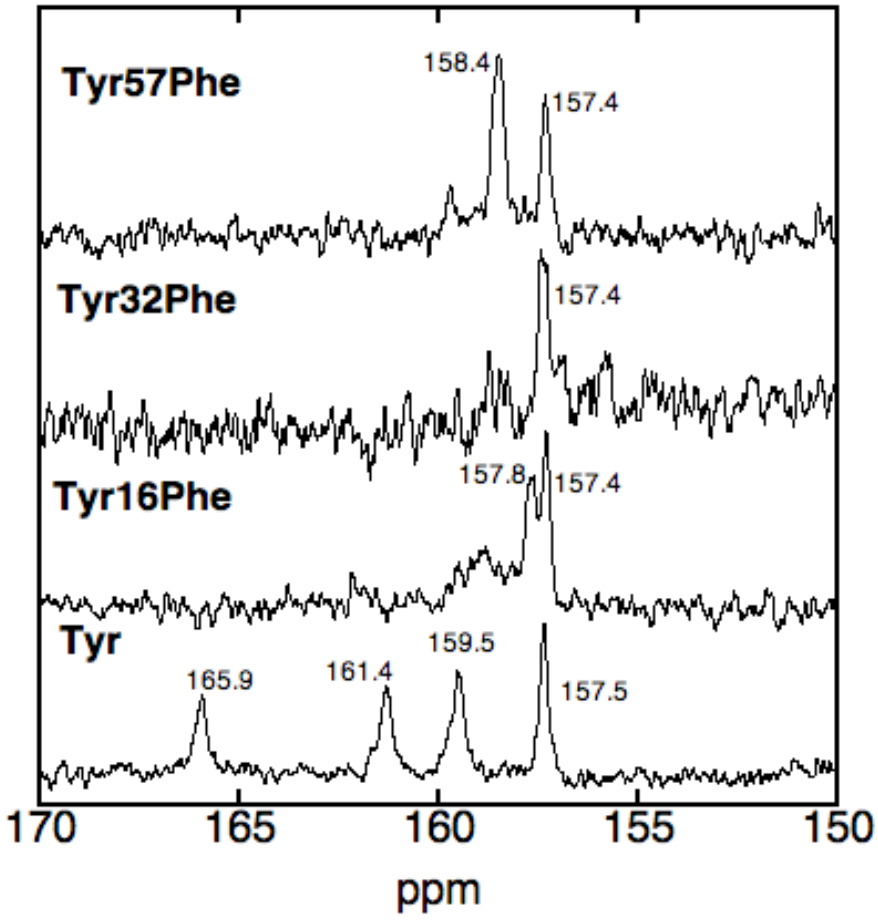

Figure S4. ^{13}C NMR spectra of Asp40Asn mutant (labeled 'Tyr') and mutants also with Tyr16Phe, Tyr32Phe, and Tyr57Phe. A peak at 165.9 ppm is not observed in the spectra for the Tyr mutants consistent with the absence of a tyrosine anion upon mutation of a nearby Tyr to Phe. Three distinct peaks were not observed in the mutants presumably due to a low signal to noise and possibly due to exchange. The UV data provide strong evidence for loss of the stabilized Tyr anion in the mutants (see main text). Spectra were collected as described in the Experimental Section.

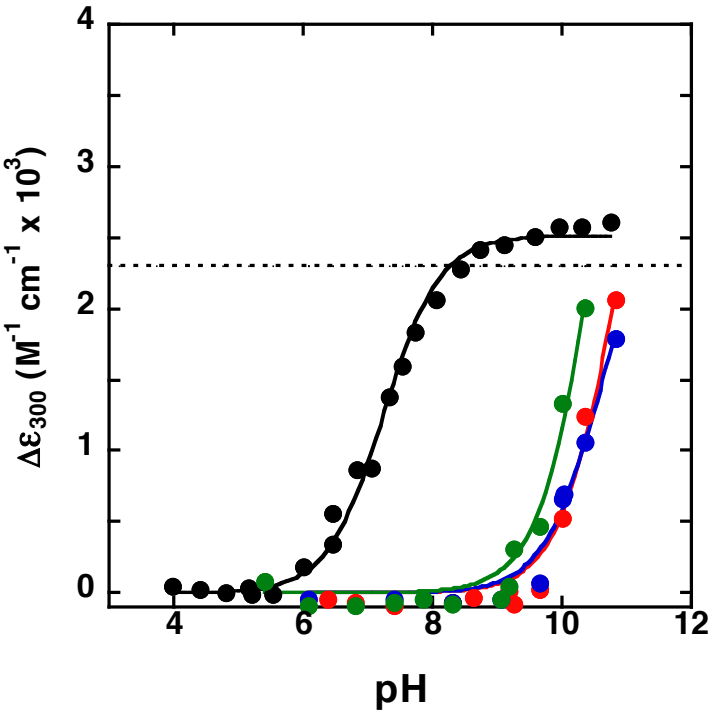

Figure S5. Changes in extinction coefficients at 300 nm relative to pH 4 for D40N (black), Y16A/D40N/D103N (red), Y32A/D40N/D103N (blue), and Y57A/D40N/D103N (green) KSI. Absorbance spectra were obtained as described in the Experimental Section. The lines are fits of the data to a titration curve, and give pK_a value of 6.5 for D40N and >10 for Y16A/D40N/D103N, Y32A/D40N/D103N, and Y57A/D40N/D103N. The increase in absorbance at 300 nm around and above pH 10 may reflect titration of more than one Tyr residue.

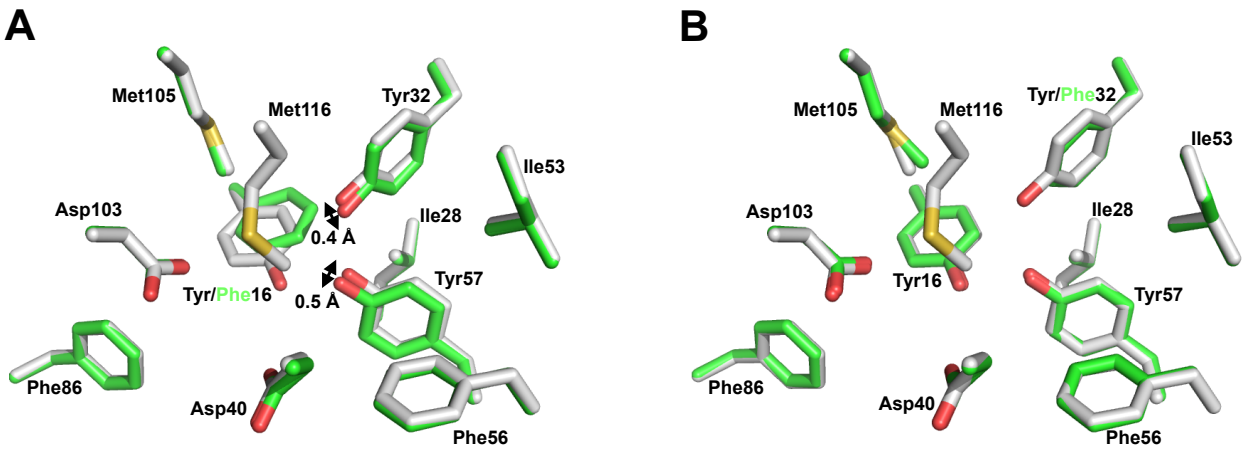

Figure S6. Effects of Tyr mutations on the position of remaining Tyr residues in the hydrogen bond network. (**A**) A previously determined crystal structure of Tyr16Phe (PDB ID 1EA2, carbon atoms colored green) shows Tyr32 and Tyr57 are displaced 0.4 and 0.5 Å, respectively, relative to wild-type KSI (PDB 1OPY, carbon atoms colored white). (**B**) A previously determined crystal structure of Tyr32Phe (PDB ID 1DMQ, carbon atoms colored green) shows that the Tyr residues are superimposable in the mutant relative to wild-type KSI (PDB 1OPY, carbon atoms colored white).

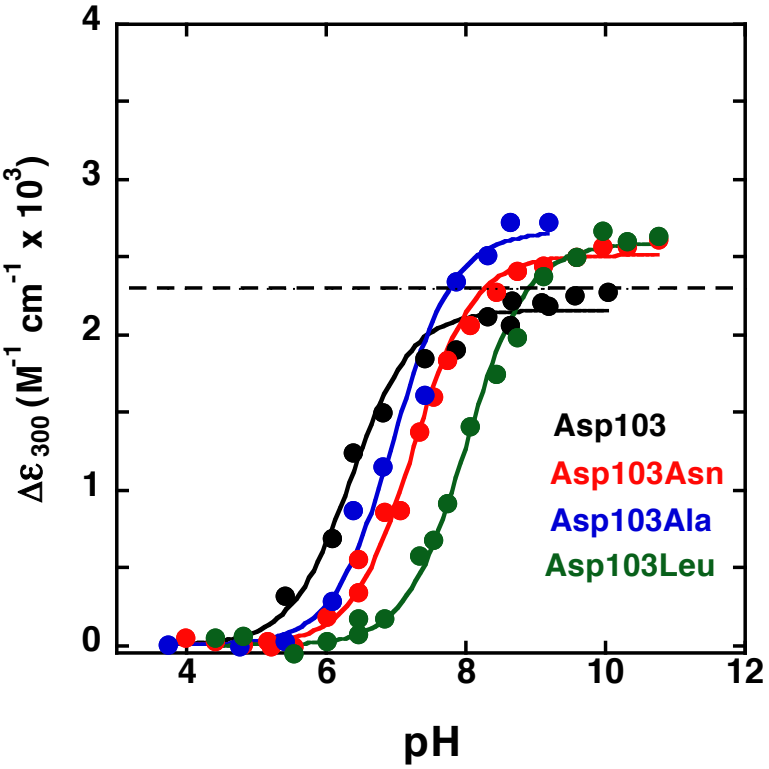

Figure S7. Changes in extinction coefficients at 300 nm relative to pH 4 for D40N (black), D40N/D103N (red), D40N/D103A (blue), and D40N/D103L (green) KSI. Absorbance spectra were collected as described in the Experimental Section. The lines are fits of the data to a titration curve, and give pK_a values of 6.3 for D40N; 7.2 for D40N/D103N; 6.9 for D40N/D103A; and 8.2 for D40N/D103L.

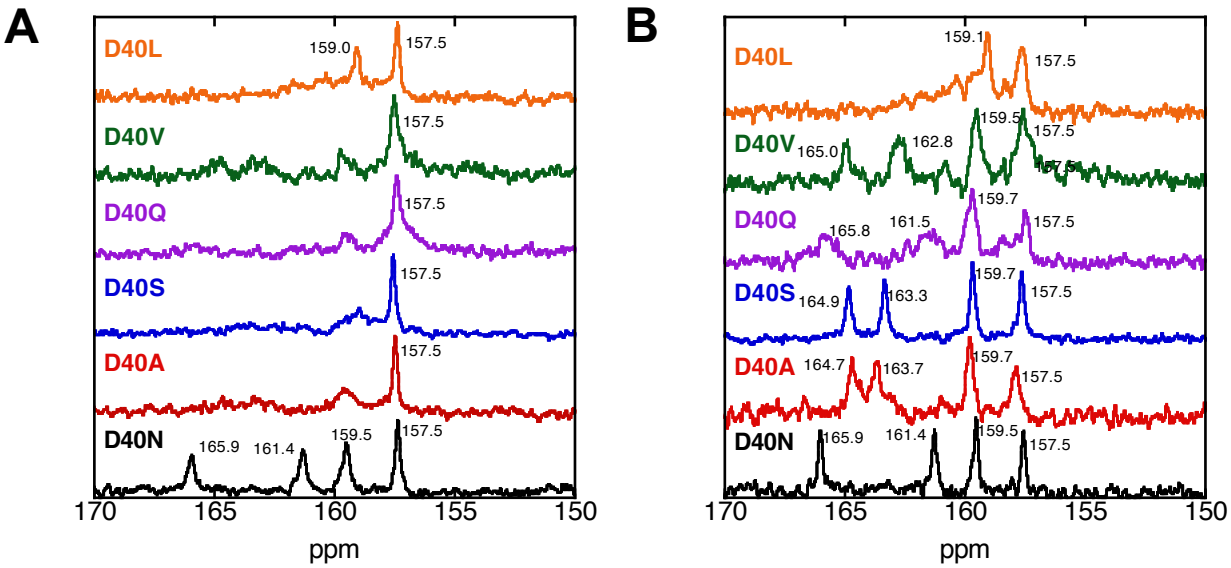

Figure S8. ^{13}C NMR spectra of Asp40 mutants (in the Asp103Asn) background at (**A**) pH 8.0 and (**B**) pH 10.0. Spectra were collected as described in the Experimental Section.

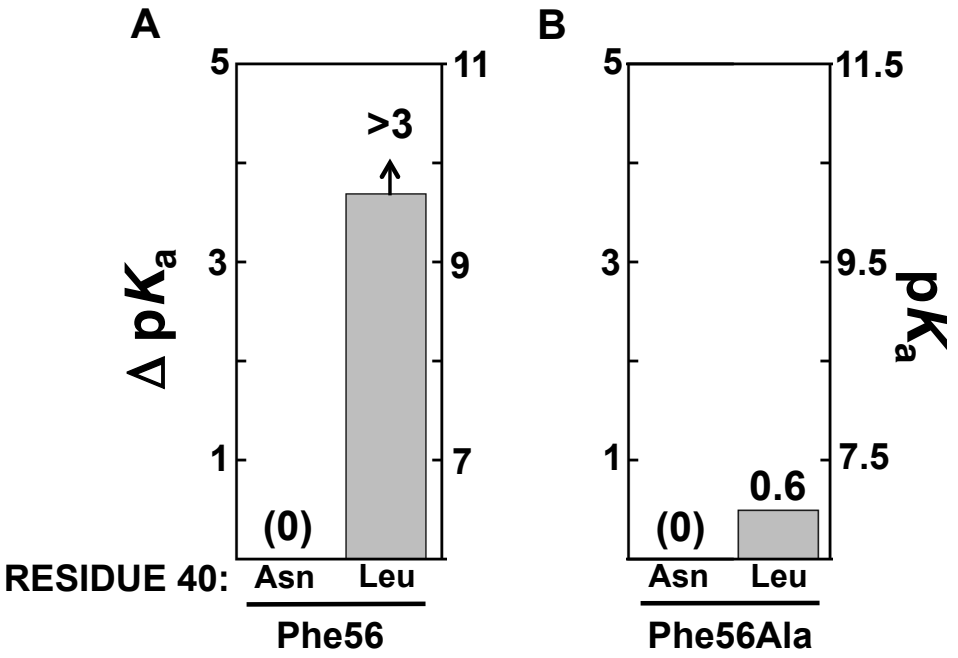

Figure S9. Effects of D40L mutations on the Tyr pK_a in the F56 and F56A backgrounds. The ΔpK_a value is relative to D40N in panel **A** and D40N/F56A in panel **B**. Values are from two or more independent measurements and are from Tables 4 and 5.

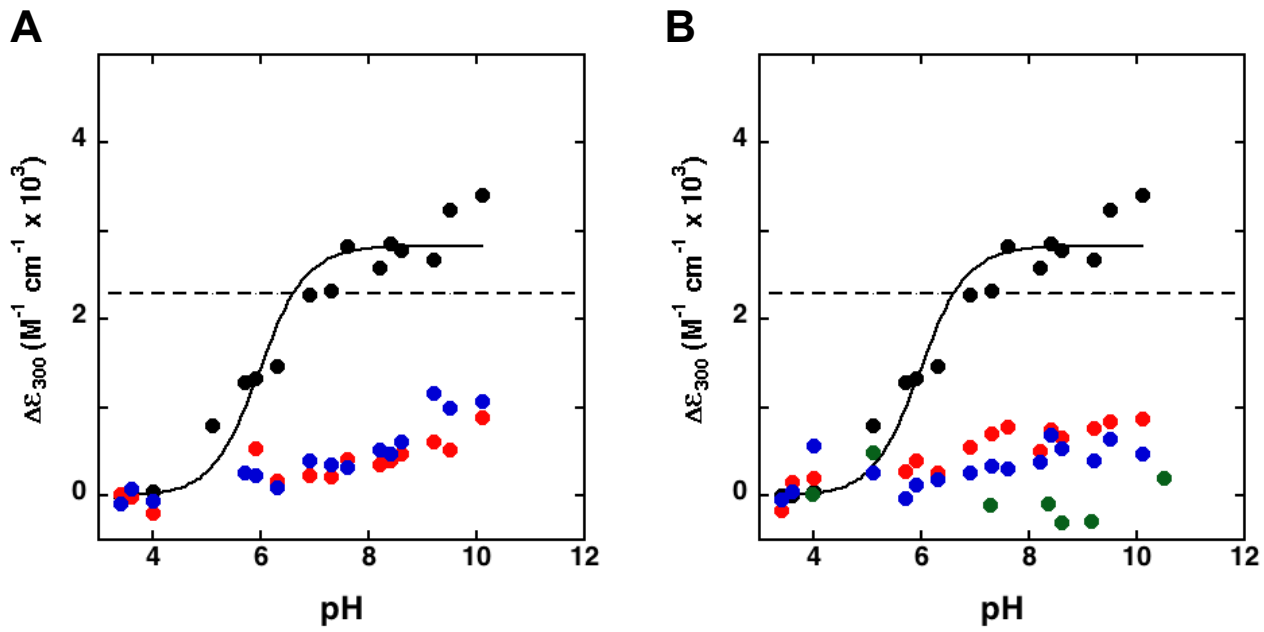

Figure S10. Changes in extinction coefficients at 300 nm relative to pH 4 for mutations of Tyr16 and Tyr32 to Phe (**A**) and Ala (**B**) in the D40R/F56A/D103A background. (**A**) Changes in extinction coefficients at 300 nm relative to pH 4 for D40R/F56A/D103A (black), Y16F/D40R/F56A/D103A (red), Y32F/D40R/F56A/D103A (blue) KSI. (**B**) Changes in extinction coefficients at 300 nm relative to pH 4 for D40R/F56A/D103A (black), Y16A/D40R/F56A/D103A (red), Y32A/D40R/F56A/D103A (blue), and Y16A/Y32A/D40R/F56A/D103A (green) KSI. Absorbance spectra were collected as described in the Experimental Section. The lines are fits of the data to a titration curve, and give a pK_a value of 6.0 for D40R/F56A/D103A.

Table S1. Tyr O•O distances in crystal structures bearing an expected tyrosine and tyrosinate at position 57.

Enzyme	PDB ID	Resolution (Å)	pH	Expected Tyr Ionization State	Chain	O•O Distance (Å) Tyr16-Tyr57	Tyr32-Tyr57	Tyr16-Tyr32
Wild type[a]	1OPY	1.9	4.6	Tyr-OH	A	2.66	2.77	4.14
D40N/M116C-CN[b]	3OXA	1.9	7.2	Tyr-O^-	A	2.63	2.60	4.23
					B	2.61	2.61	4.22
					C	2.57	2.57	4.20
					D	2.59	2.60	4.20
Average Tyr O•O distance in D40N/M116C-CN structure						2.60	2.60	4.21

[a]While KSI is a dimer, only one monomer chain is available in the wild-type structure file.

[b]The D40N/M116C-CN structure contains four monomer chains in the structure file.

Table S2. Crystallographic Data Collection and Refinement Statistics		
Data Set	**pKSI M116A**	**tKSI D40H/D103N** [a]
PDB ID	3RGR	3MYT
Resolution Range (Å)	33.5-1.59 (1.68-1.59)[b]	29.9-2.00 (2.05-2.00)[b]
Space Group	$C222_1$	$P6_122$
a, Å	35.8	64.04
b, Å	94.7	64.04
c, Å	72.4	502.22
α, °	90.0	90.0
β, °	90.0	90.0
γ, °	90.0	120.0
Number Unique Reflections	16562 (2114)	43283 (5933)
Completeness	98.0 (87.3)	99.6 (97.3)
Multiplicity	4.0 (3.3)	26.4 (21.4)
R_{merge}, %	6.6 (56.6)	16.7 (23.5)
I/σ	14.1 (2.2)	21.8 (4.7)
Refinement Statistics		
No. Residues	128	124
No. Waters	94	398
R_{work}, %	18.7 (28.7)	16.7 (23.5)
R_{free}, %	24.3 (33.6)	21.3 (29.8)
rmsd bond, Å	0.022	0.026
rmsd angle, °	2.0	1.96

$R_{merge}=\Sigma_{hkl}\Sigma_i|I(hkl)_i-\{I(hkl)\}|/\Sigma_{hkl}\Sigma_i I(hkl)_i$

$R_{work}=\Sigma_{hkl}|F(hkl)_o-\{F(hkl)_c\}|/\Sigma_{hkl}F(hkl)_o$

R_{free} was calculated exactly as R_{work} where $F(hkl)_o$ were taken from 10% of the data not included in refinement.

[a] For simplicity, pKSI numbering is used throughout.

[b] Highest resolution shell is in parentheses.

Table S3. Tyrosine residues with unusually low pK_a values reported in the literature

Enzyme	Tyr	Tyr pK_a	Reported basis for stabilization of tyrosine anion
Alanine racemase (*1*)	Tyr265	7.5	Arg219
UDP-galactose 4-epimerase (*2*)	Tyr149	6.4	NAD^+, Lys153, Ser124
dTDP-glucose 4,6-dehydratase (*3*)	Tyr160	6.4	Lys164, Thr134
Calmodulin (*4*)	Tyr99	7.0	Ca^{2+}

Table S4. Summary of the effects of mutations on the Tyr pK_a

Protein	pK_a	Δ pK_a	Protein	pK_a	Δ pK_a
D40N	6.3	(0)	D40A D103A	8.7	2.4
D40 (wild type)	>10	>3	D40N F56A	6.9	0.6
D40A	7.1	0.8	D40N M86A	6.3	0
D40L	>10	>3	D40N M105A	6.3	0
D40N D103N	7.2	0.9	D40N M116A	5.9	-0.4
D40N D103A	6.9	0.6	F56A	9.0	2.7
D40N D103L	8.2	1.9	D40A F56A	6.8	0.5
Y16F D40N D103N	>10	>3	D40R F56A	6.8	0.5
Y57F D40N D103N	>10	>3	F56A D103N	9.8	3.5
Y32F D40N D103N	>9	>2	F56A D103A	10	3.7
Y16A D40N D103N	>10	>3	D40E F56A D103N	9.8	3.5
Y57A D40N D103N	>10	>3	D40R F56A D103A	5.9	-0.4
Y32A D40N D103N	>10	>3	D40A F56A D103A	8.1	1.8
D40A D103N	8.3	2.0	D40N F56A D103A	8.1	1.8
D40S D103N	8.2	1.9	D40N F56A D103N	7.4	1.1
D40V D103N	8.5	2.2	Y16F D40R F56A D103A	>10	>3
D40I D103N	8.6	2.3	Y32F D40R F56A D103A	>10	>3
D40Q D103N	7.9	1.6	Y16A D40R F56A D103A	>10	>3
D40L D103N	>10	>3	Y32A D40R F56A D103A	>10	>3
D40E D103N	>10	>3	Y16A Y32A D40R F56A D103A	>10	>3
D40H D103N	8.8	2.5			
D40K D103N	9.2	2.9			
D40R D103N	8.2	1.9			

pK_a values determined at 25 °C, in 10 mM buffer. Average of two or more replicates; standard deviation ±0.2. ΔpK_a values are relative to D40N. For simplicity, pKSI numbering is used throughout.

Supporting Information References.

1. Sun, S., and Toney, M. D. (1999) Evidence for a two-base mechanism involving tyrosine-265 from arginine-219 mutants of alanine racemase, *Biochemistry 38*, 4058-4065.
2. Liu, Y., Thoden, J. B., Kim, J., Berger, E., Gulick, A. M., Ruzicka, F. J., Holden, H. M., and Frey, P. A. (1997) Mechanistic roles of tyrosine 149 and serine 124 in UDP-galactose 4-epimerase from Escherichia coli, *Biochemistry 36*, 10675-10684.
3. Gerratana, B., Cleland, W. W., and Frey, P. A. (2001) Mechanistic roles of Thr134, Tyr160, and Lys 164 in the reaction catalyzed by dTDP-glucose 4,6-dehydratase, *Biochemistry 40*, 9187-9195.
4. Pundak, S., and Roche, R. S. (1984) Tyrosine and tyrosinate fluorescence of bovine testes calmodulin: calcium and pH dependence, *Biochemistry 23*, 1549-1555.